Hindawi Publishing Corporation
International Journal of Photoenergy
Volume 2012, Article ID 962649, 6 pages
doi:10.1155/2012/962649

Research Article

Tailoring the Composition and Properties of Sprayed $CuSbS_2$ Thin Films by Using Polymeric Additives

Ionut Popovici and Anca Duta

Department of Renewable Energy Systems and Recycling, Transilvania University of Brasov, Eroilor 29, 500036 Brasov, Romania

Correspondence should be addressed to Anca Duta, a.duta@unitbv.ro

Received 21 June 2011; Accepted 1 November 2011

Academic Editor: Vincenzo Augugliaro

$CuSbS_2$ thin films were obtained by spray pyrolysis deposition, using polymeric additives for controlling the surface properties and film's composition. Ternary crystalline chalcostibite compounds have been obtained without any postdeposition treatments. XRD spectra and IR spectroscopy were used to characterize films composition and interactions between components. Films morphology and surface energy were investigated using AFM microscopy and contact angle measurements. Hydrophobic and hydrophilic polymers strongly influence the composition and film morphology.

1. Introduction

In heterojunction devices (solar cells), copper-based absorbers have been intensively studied mainly for their p-type conductivity due to copper deficiency [1]. More recently, ternary CIS/CIGS compounds with Cu(In/Ga/Sb/Bi)(S/Se) structures were investigated as candidates in non-silicon solar cell application. The In^{3+} or Ga^{3+} ions in the lattice reduce the Cu^{+} ions mobility thus increasing the stability comparing to the copper sulfides ($Cu_{2-x}S$). Most of the studies are focused on $Cu(In, Ga)(S/Se)_2$ while antimony-based compounds are less reported. In this paper $CuSbS_2$ (chalcostibite) thin films are investigated as an alternative absorber, because of the similar properties required for photovoltaic materials, with the advantage that antimony has a lower purchase price than indium. Also, copper-gold structures that reduce the CIS/CIGS efficiency were not reported for the antimony compound.

The first report on chalcostibite occurrence came from Rhar-el-Anz in Morocco/Tunisia in 1942 as a mineral of dark gray color with metallic luster, [2], with an orthorhombic [JCPDS 44-1417] crystal structure. In terms of structural properties, $CuSbS_2$ is often formed as a mixture of different phases also including Sb_2S_3 [3], or Cu_3SbS_3, and Cu_3SbS_4 [1, 4].

Literature reports on its synthesis using different techniques, both in crystalline and amorphous state. Amorphous $CuSbS_2$ was obtained from vacuum postgrowth treatments of single-source thermal evaporation films, with optical transition in the range 1.8–2 eV [3]. Crystalline $CuSbS_2$ was obtained by hydrothermal synthesis at 200°C [5] with similar structure as the natural mineral (JCPDS 35-413) and congruent crystallization at 552°C [1]. There are other various deposition techniques reported for obtaining crystalline $CuSbS_2$ thin films, with variable properties in terms of crystallinity, phase composition, and morphologies: chemical bath deposition, [6], single-source thermal evaporation method [3, 7], solvothermal growth [8], and sputtering [9]. Thin films of $CuSbS_2$ with different morphologies, varying from brick-like to plank-like, fibbers [10], and spherical morphology are reported to be obtained using spray pyrolysis deposition [8, 10, 11].

Crystalline $CuSbS_2$ thin films (direct band-gap 1.52 eV and p-type conductivity) have been used in solid state solar cells with the structure: $FTO/CdS/Sb_2S_3/CuSbS_2$ [12], $FTO/TiO_2/CuSbS_2/C$ [11], and $TCO/CdS/Sb_2S_3/Sb_2S_3$-CuS ($CuSbS_2$)/Ag [6]. One of the main limitations in the cells efficiency is imposed by the contact at the interface between the n-type and p-type semiconductors. Therefore, there is a strong need for tailoring the thin films morphology,

Table 1: Precursor solution composition.

Sample	$CuCl_2 \cdot 2H_2O$ mmol	$(CH_3COO)_3Sb$ mmol	H_2NCSNH_2 mmol	Cu : Sb : S molar ratio
A	0.81	1.2	10.5	1 : 1.48 : 13
B	0.81	1.6	10.5	1 : 1.97 : 13
C	0.81	2	10.5	1 : 2.48 : 13
D	0.81	2.81	10.5	1 : 3.47 : 13
E	0.81	3.81	10.5	1 : 4.4 : 13
F	0.87	1.6	10.5	1 : 1.84 : 13
G*	0.87	1.6	10.5	1 : 1.84 : 13
H**	0.87	1.6	10.5	1 : 1.84 : 13

* Polymer additive: HFL-100 ppm.
** Polymer additive: HFB-100 ppm.

supporting a good reciprocal infiltration, and avoiding shunts.

The morphology of the thin layers depends on the deposition conditions, with influence on the ratio between the nucleation and growth rates (e.g., high nucleation/growth ratio results in small grains, dense films). These rates are correlated with the reaction affinity of the precursors' species which, in turn, depends on their stability. The control of the reactants stability in the precursors' solution can be reached using additives able to form physical or chemical bonds with the precursor ions. The usually mentioned additives are low-molecular organic compounds (with OH and C=O groups). Their use, although efficient, can rise toxicity and cause problems. The use of polymers, with variable hydrophobic degree, represents a novel alternative investigated in this paper.

Considering the multilayered structure of a solid state solar cell, another important aspect governing the reciprocal infiltration is a good adherence of the precursor on the host layer, developed as a high energy surface. Therefore, the influence of polymeric additives on the surface properties of the $CuSbS_2$ films is also reported.

2. Experimental

2.1. Deposition Part. $CuSbS_2$ thin films were deposited by spray pyrolysis deposition on an automatic installation, on FTO (fluorine-doped thin oxide, TEC 8/3 mm Pilkington) conductive glass. The glass was washed in an ultrasonic bath, in several immersions in alcohol and then dried with compressed air. The glass was heated at the deposition temperature on a thermostatic heating plate. As precursors, aqueous solutions of copper(II)-chloride dehydrate, (Scharlau, $CuCl_2 \cdot 2H_2O$, min 99%), concentration between 16.2–17.4 mM, antimony(III) acetate, (Alfa Aesar, $(CH_3COO)_3Sb$, 99.99%), concentration between 24–76.2 mM, and thiourea, concentration 210 mM, (Scharlau, H_2NCSNH_2, 99%) were prepared, with a small addition of HCl for insuring the solubility of the antimony acetate. Two polymeric additives, sodium maleate-methyl metacrylate (hydrophilic polymer, HFL) and sodium maleate-vinyl acetate (hydrophobic polymer, HFB) were used, completing the complexion effect of thiourea.

Thin films, with different composition and morphology were obtained by varying the precursors' concentrations and molar ratio between components, as presented in Table 1.

For samples G and H polymeric additives were used in 100 ppm concentration.

Previously optimized deposition parameters [11] were used for all the samples: temperature of 240°C, carrier gas (air) pressure of 1.5 bar, spraying height 25 cm, with 60 seconds pause between two spraying sequences.

2.2. Film Characterization. The $CuSbS_2$ films deposited on FTO were analyzed using X-ray diffraction (XRD, Bruker-AXS-D8, $Cu_{K\alpha 1}$ radiation) and atomic force microscopy (AFM/STM, NT-MDT model NTEGRA Probe Nanolaboratory), in semicontact mode, with an Si-tip (CSG10, force constant 0.15 N/m, tip radius10 nm); surface energy and wetting properties were analyzed using the Sessile drop technique for contact angle measurements with a OCA-20 Contact Angle-meter (DataPhysics Instruments). The IR reflectance spectra were recorded with a Spectrum BX FT-IR System (Perkin Elmer).

3. Results and Discussions

At the selected deposition parameters, all films presented a smooth homogenous aspect.

The diffraction analysis of the films show the formation of crystalline $CuSbS_2$ (PDF 00-009-0143) in orthorhombic polymorph, along with famatinite Cu_3SbS_4 (PDF 00-035-0581), proving that spray pyrolysis can be used as deposition method for crystalline ternary Cu-Sb-S thin films. The Cu_3SbS_4 pattern in the XRD spectra of chalcostibite films was also obtained and explained by Rodríguez-Lazcano et al. as the result of copper sulfide excess which leads to the formation of copper-rich Cu-Sb-S compounds [1]. Literature [1] mentions that antimony in excess can further form binary sulphides either crystalline or amorphous. Still, the results show that, in our experimental conditions, even in Sb-excess precursors only ternary stable compounds are formed and not mixtures of secondary sulphides.

The deposition temperature assures enough thermal energy for the two main processes that take place on the substrate surface: first, the evaporation of solvents and breaking

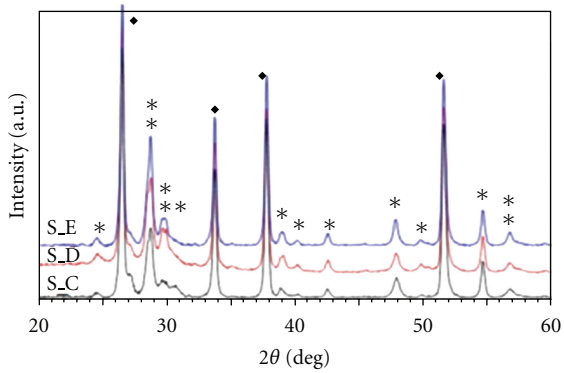

Figure 1: XRD spectra recorded for samples C, D, E.

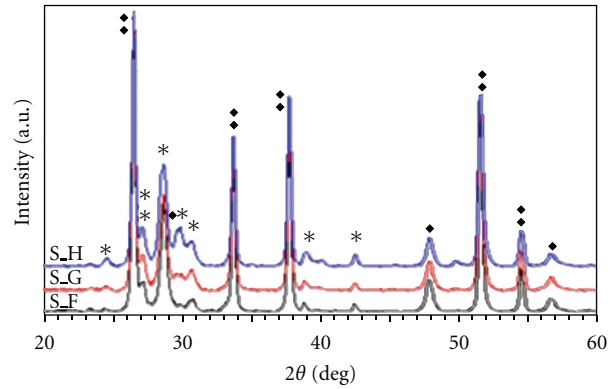

Figure 2: XRD spectra recorded for samples F, G, H.

of the chemical bounds in the precursors, followed by nucleation and crystal growth.

Because evaporation of solvents takes place/very/close to the substrate surface, regions with lower temperatures are temporarily created. Thus, an important factor is the pause between the spraying sequences that must be long enough to allow the substrate reheating and the formation of nucleation centers.

The XRD spectra of the C, D, and E samples are presented in Figure 1. Since the films are very thin, the XRD spectrum of tin dioxide SnO_2 (PDF 01-077-0451) from the FTO substrate is also visible.

Figure 2 presents the XRD pattern for F, G, and H samples, having the same precursor solution composition in which polymeric additives were used. At this precursor molar ratio in the solution, a new phase is detected in the XRD pattern, copper antimony sulphide, Cu_3SbS_3 (PDF 01-088-1335). The XRD spectra of these films do not indicate carbon in crystalline form as a residue from the polymers, while amorphous carbon based compounds are in small amounts, as shown in the FTIR spectra. This indicates that the deposition temperature is high enough for the almost total degradation of the organic polymers, forming volatile compounds.

Using the Scherrer's formula, the crystallite dimensions were estimated and are presented for the Cu-Sb-S phases identified in the A–H samples in Table 2.

3.1. Samples without Polymeric Additives. For samples A, B, and F, where the Cu : Sb precursor ratio is under 1 : 2, the Sb content influences both the nucleation and growth rate, this can be deduced form the large differences in the crystallite size and their proportion in the two phases. For sample, F it was registered also a new phase Cu_3SbS_3. For samples C, D, and E, where the Cu : Sb precursor ratio is between 1 : 2.48–1 : 4.4, the Sb content variation influences only the nucleation rate. The data shows that the crystallite size of the two phases is almost equal for each sample. The nucleation speed for sample D is the largest of the samples presented, resulting in a large number of crystals with the smaller dimensions.

3.2. Samples with Polymeric Additives. The crystallite size of the Cu_3SbS_3 phase varies in a large range as result of the polymer complexion effect on the film formation rate, (films F, G, and H). This influence is registered only for the Cu_3SbS_3 phase, the $CuSbS_2$ and Cu_3SbS_4 crystallite sizes remaining almost constant for the three samples. This could be the result of a more sensitive synthesis reaction of Cu_3SbS_3, when the influence of the polymer-precursor interactions becomes significant. The crystallite sizes of this compound are much larger than the corresponding values for $CuSbS_2$, and Cu_3SbS_4, therefore, we can conclude that there is a lower nucleation rate (more stable polymer-precursors intermediates) and/or a fast growth rate for Cu_3SbS_3. The samples with polymers contain a smaller amount of $CuSbS_2$ and a larger amount of Cu_3SbS_4 than the sample with the same composition and no additive, indicating that competitive reactions are running and the reaction affinity is influenced by the polymers.

Infra-red reflectance spectra were recorded for samples F, G, H, Figure 3, looking for residual carbon (crystalline or amorphous) from the polymer that can be additionally found in the films.

The spectra give few clues to the reaction mechanism and the processes that take place in the solutions. The functional groups from the urea compounds, NH_2, C–N, C–N–H, N–H can be found at 1400, 1500, 1620, 2068, 3350, and 3800 nm [13]. Peaks observed at 702 and 1200 nm are attributed to C=S groups from the thiourea. The vibration at 2350 nm, attributed to O=C=O, can be found only for samples G and H, being related to the polymers composition as trapped or adsorbed compound. The peaks present at 1711 and 1768 nm are assigned to the COO^- and C=O groups from the maleic anhydride. At 2880 a peak can be attributed to an S–CH_3 group.

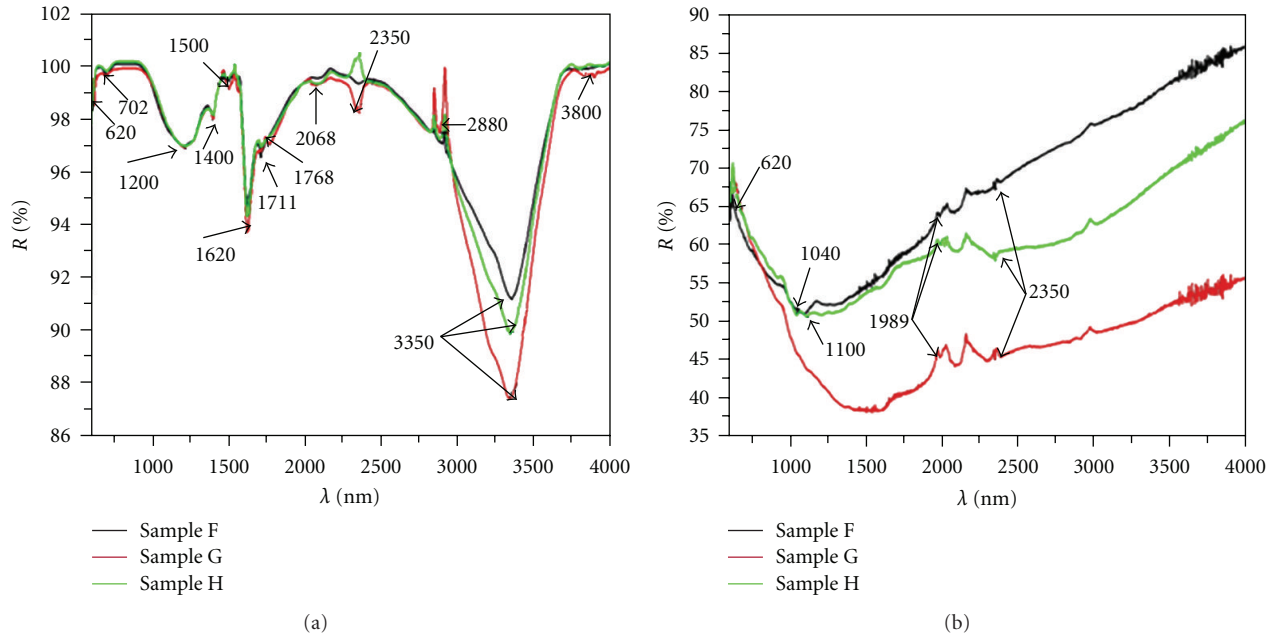

Figure 3: FTIR reflectance spectra for samples F, G, H: (a) for films, (b) for precursor solution.

Table 2: Crystallite size and phase composition for samples A–H.

Sample	Phase composition (%)			Crystallite size (Å)		
	Cu_3SbS_4	$CuSbS_2$	Cu_3SbS_3	Cu_3SbS_4	$CuSbS_2$	Cu_3SbS_3
A	34.2	65.8	—	236.1	143.1	—
B	78	22	—	236.1	161.5	—
C	30	70	—	181.9	180.1	—
D	27	73	—	146.3	164.7	—
E	34	66	—	217.3	216.2	—
F	67	28	5	196.3	171.5	352
G	82	11	7	172.4	173.8	577.7
H	82	11	7	159.4	160.7	268.8

The peak at 620 nm, was assigned to Cu_2O [13], in the solution spectra and is found both in the precursors and in the thin films. In the film, the copper oxide however is believed to be in amorphous form because it does not appear in the XRD spectra of the samples.

In the films, the IR peaks positioned at 1989 nm were attributed to C–C groups, and the vibrations found at 1040 and 1110 nm are associated with copper thiourea complexes [14].

The carbon traces revealed in the films by the FTIR analysis, as CO_2 and other C–C groups were not detected by the XRD analysis, confirming the amorphous structures.

Thus, the films contain very low amount of amorphous inorganic phases (Cu_2O) and traces of organic compounds resulted in the thermal decomposition of the polymeric additives.

The morphology of the deposited samples was investigated and the AFM images (Figures 4(a)–4(e)) of the films show the effect of the precursor solution composition and of the polymeric additives.

In Figures 4(a) and 4(b), the AFM images recorded for samples B and D are presented. Sample B presents a multigrain structure with open, micropores, that can have a positive effect on the reciprocal infiltration of the n and p-type semiconductors in the solid state solar cells. The increase in the antimony content leads to the extension of the grains into fibber-like aggregates.

The AFM images recorded for samples F, G, and H are presented in Figures 4(c)–4(e). The use of polymeric additives increases the density of the films. The worm-like structures obtained for sample F tend to bind together and form denser structures in the films were polymeric additives were used. Also a decrease in grain size is observed in these samples. Correlating these results with the XRD data we can assume that the larger crystallites, with regular geometry, are able to (slowly) grow in dense structures, this effect being more evident when the hydrophilic polymer is used.

Contact angle measurements were used to calculate the surface energy of the samples. Because solid state solar cells are constructed by the infiltration of the n and p-type

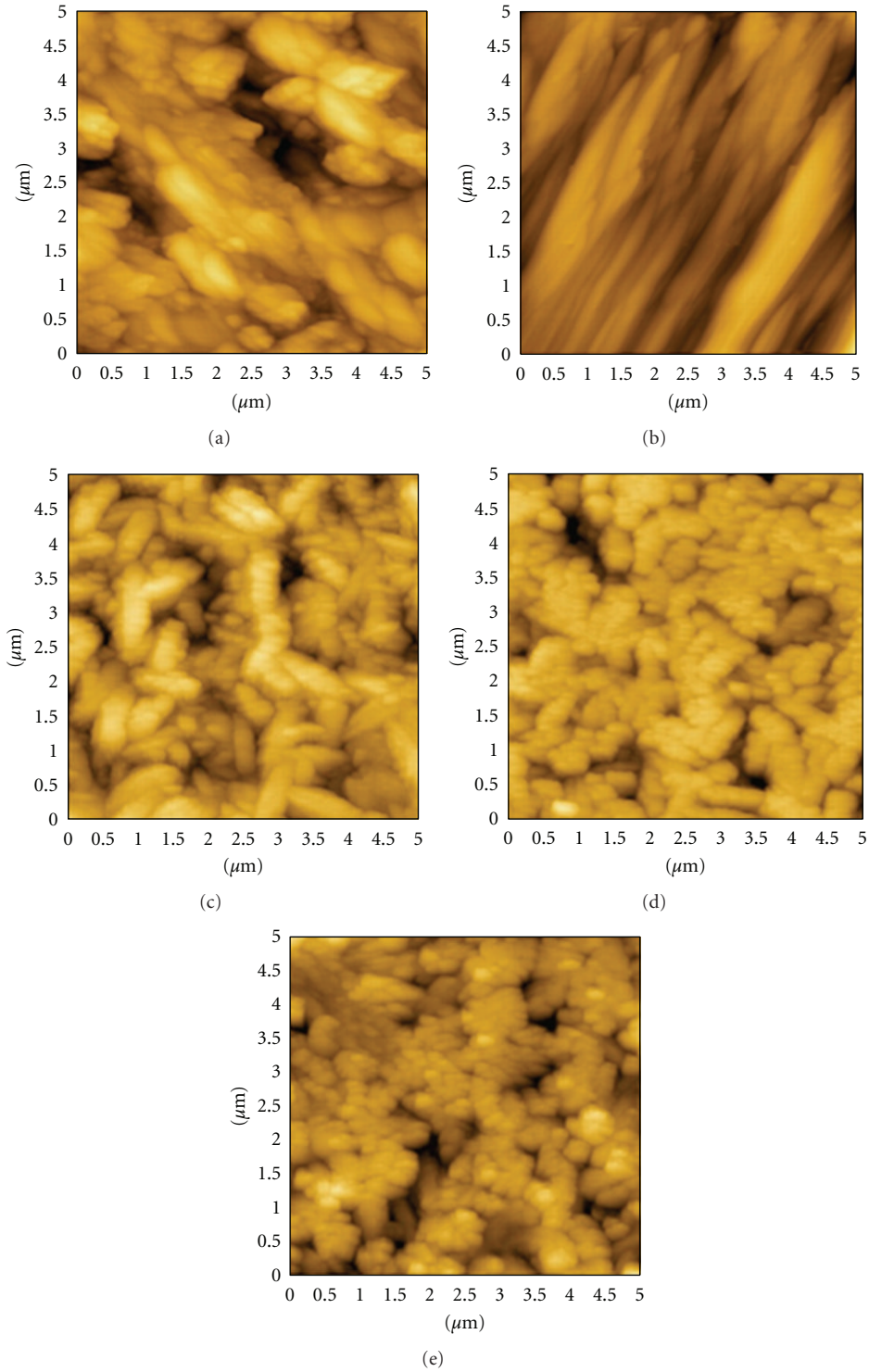

Figure 4: AFM image of sample B (a), E (b), F (c), G (d), and H (e) at $5 \times 5\,\mu$m resolution.

semiconductors, a good contact between the semiconductors is essential. During SPD, deposition takes place from liquid, aqueous solutions; this is why substrates with high surface energy and good wetting capabilities are required. The contact angle measurements were carried out using two liquids: water and glycerol. With the value of the initial contact angles, energy surface was calculated using Owens, Wendt and Kaelble method [15]. The data are presented in Table 3.

When using glycerol, with low polarity, all the substrates show large and similar contact angle values, corresponding to polar, partially charged, substrates.

Table 3: Contact angles and surface energies measured for samples F, G, and H.

Sample	Additive, 100 ppm	Θ water (degree)	Θ glycerol (degree)	Surface energy (mN/m)	Dispersive component (mN/m)	Polar component (mN/m)	Roughness, measured on $20 \times 20\,\mu$m (nm)
F	—	111	107.5	7.81	3.88	3.93	193
G	HFL	93.5	103.3	23.33	0	23.33	138
H	HFB	78	104.3	74.46	8.13	64.33	152

The contact angles measured for water (with much higher polarity) allow us to sense the differences among the ionic degree of the samples. By using polymeric additives (samples G and H), a decrease in the initial contact angle is observed, in comparison with sample F. This gets the conclusion that polymers also have influence on the surface charge distribution, as result of changing the nucleation and growth ratios. With a contact angle value below 90°, sample H has the best wetting capacity and the largest surface energy from the three samples. The surface roughness can also influence the contact angle (being lower for rough surfaces). It is interesting also to notice the very low dispersive component of the surface energy in sample G (registered as "0") proving that the hydrophilic polymer supports the formation of rather dense, ionic layers.

4. Conclusions

Thin films of crystalline Cu-Sb-S ternary compounds were obtained on FTO substrate using spray pyrolysis deposition technique, without any postdeposition treatments. Films containing $CuSbS_2$, Cu_3SbS_4, and Cu_3SbS_3 phases were prepared by varying the precursors' composition. Evidences of traces of amorphous carbon-based compounds were recorded in the FTIR spectra, for the samples using polymer additives.

The samples morphology can be varied from multigrain, open pores up to long fiber-like aggregates, and to smaller worm-like morphologies. The use of polymeric additives results in a densification of the films and a decrease in the grain size, containing large crystallites of Cu_3SbS_3.

The polymeric additives represent a powerful tool also in tuning the surface energy, thus increasing the wetting behavior, as a prerequisite for developing efficient n-p junctions in solid state solar cells.

Acknowledgment

This work was supported by CNCSIS_UEFISCDI Project no. PNII-IDEI 840/2008, Romania.

References

[1] Y. Rodríguez-Lazcano, M. T. S. Nair, and P. K. Nair, "$CuSbS_2$ thin film formed through annealing chemically deposited Sb_2S_3-CuS thin films," *Journal of Crystal Growth*, vol. 223, no. 3, pp. 399–406, 2001.

[2] G. A. Harcourt, "Tables for identification of ore minerals by X-ray powder patterns," *American Mineralogist*, vol. 27, p. 63, 1942.

[3] A. Rabhi, M. Kanzari, and B. Rezig, "Growth and vacuum post-annealing effect on the properties of the new absorber $CuSbS_2$ thin films," *Materials Letters*, vol. 62, no. 20, pp. 3576–3578, 2008.

[4] Y. Rodríguez-Lazcano, L. Guerrero, O. Gomez Daza, M. T. S. Fair, and P. K. Nair, "Antimony chalcogenide thin films: chemical bath deposition and formation of new materials by post deposition thermal processing," *Superficies y Vacio*, vol. 9, pp. 100–103, 1999.

[5] I. L. Lind and E. Makovicky, "Phase relations in the system Cu-Sb-S at 200oC, 10^8 Pa by hydrothermal synthesis. Microprobe analyses of tetrahedrite—a warning," *Neues Jahrbuch fur Mineralogie, Abhandlungen*, vol. 145, pp. 134–156, 1982, as cited in JCPDS 35-0413.

[6] S. Messina, M. T. S. Nair, and P. K. Nair, "Antimony sulfide thin films in chemically deposited thin film photovoltaic cells," *Thin Solid Films*, vol. 515, no. 15, pp. 5777–5782, 2007.

[7] A. Rabhi, M. Kanzari, and B. Rezig, "Optical and structural properties of $CuSbS_2$ thin films grown by thermal evaporation method," *Thin Solid Films*, vol. 517, no. 7, pp. 2477–2480, 2009.

[8] J. Zhou, G.-Q. Bian, Q.-Y. Zhu, Y. Zhang, C.-Y. Li, and J. Dai, "Solvothermal crystal growth of $CuSbQ_2$ (Q=S, Se) and the correlation between macroscopic morphology and microscopic structure," *Journal of Solid State Chemistry*, vol. 182, no. 2, pp. 259–264, 2009.

[9] M. Y. Versavel and J. A. Haber, "Structural and optical properties of amorphous and crystalline antimony sulfide thin-films," *Thin Solid Films*, vol. 515, no. 18, pp. 7171–7176, 2007.

[10] S. Manolache, A. Duta, L. Isac, M. Nanu, A. Goossens, and J. Schoonman, "The influence of the precursor concentration on $CuSbS_2$ thin films deposited from aqueous solutions," *Thin Solid Films*, vol. 515, no. 15, pp. 5957–5960, 2007.

[11] S. A. Manolache and A. Duta, "The influence of the spray deposition parameters in the photovoltaic response of the three-dimensional (3D) solar cell: TCO/dense TiO_2/$CuSbS_2$/graphite," *Journal of Optoelectronics and Advanced Materials*, vol. 9, no. 10, pp. 3219–3222, 2007.

[12] Y. Rodríguez-Lazcano, M. T. S. Nair, and P. K. Nair, "Photovoltaic p-i-n structure of $Sb2S_2$ and $CuSbS_2$ absorber films obtained via chemical bath deposition," *Journal of the Electrochemical Society*, vol. 152, no. 8, pp. G635–G638, 2005.

[13] K. Das, S. K. Panda, S. Gorai, P. Mishra, and S. Chaudhuri, "Effect of Cu/In molar ratio on the microstructural and optical properties of microcrystalline $CuInS_2$ prepared by solvothermal route," *Materials Research Bulletin*, vol. 43, no. 10, pp. 2742–2750, 2008.

[14] P. Bombicz, I. Mutikainen, M. Krunks, T. Leskelä, J. Madarász, and L. Niinistö, "Synthesis, vibrational spectra and X-ray structures of copper(I) thiourea complexes," *Inorganica Chimica Acta*, vol. 357, no. 2, pp. 513–525, 2004.

[15] D. K. Owens and R. C. Wendt, "Estimation of the surface free energy of polymers," *Journal of Applied Polymer Science*, vol. 13, no. 8, pp. 1741–1747, 1969.